E3S Web of Conferences **4**, 03003 (2014)
DOI: 10.1051/e3sconf/20140403003

Neutron background estimates in GESA

A.C. Fernandes[1,2], M. Felizardo[2], T.A. Girard[2,3], A. Kling[1,2], A.R. Ramos[1,2], J.G. Marques[1,2], M.I. Prudêncio[1], R. Marques[1] and F.P. Carvalho[1]

[1] Centro de Ciências e Tecnologias Nucleares, Instituto Superior Técnico, Universidade de Lisboa, E.N. 10 (km 139.7), 2695-066 Bobadela, Portugal
[2] Centro de Física Nuclear, Universidade de Lisboa, 1649-003 Lisboa, Portugal
[3] Department of Physics, Universidade de Lisboa, 1749-016 Lisboa, Portugal

Abstract. The SIMPLE project looks for nuclear recoil events generated by rare dark matter scattering interactions. Nuclear recoils are also produced by more prevalent cosmogenic neutron interactions. While the rock overburden shields against (μ,n) neutrons to below $10^{-8}\,\mathrm{cm}^{-2}\,\mathrm{s}^{-1}$, it itself contributes via radio-impurities. Additional shielding of these is similar, both suppressing and contributing neutrons. We report on the Monte Carlo (MCNP) estimation of the on-detector neutron backgrounds for the SIMPLE experiment located in the GESA facility of the Laboratoire Souterrain à Bas Bruit, and its use in defining additional shielding for measurements which have led to a reduction in the extrinsic neutron background to $\sim 5 \times 10^{-3}$ evts/kgd. The calculated event rate induced by the neutron background is $\sim$0,3 evts/kgd, with a dominant contribution from the detector container.

1. Introduction

The SIMPLE detectors and experiment are extensively described in the literature [1]. The superheated liquid C_2ClF_5 droplets within a gel matrix vaporize upon energy absorption from radiation having Linear Energy Transfer (LET) $>150\,\mathrm{keV}/\mu\mathrm{m}$; the phase transition produces a characteristic sound that is recorded and identified as an event.

In general, only neutron-generated recoils, α's and dark matter interactions are capable of providing the necessary LET. Neutrons originate from spontaneous fission and (α,n) reactions induced by the decay of ^{238}U and ^{232}Th contaminants in GESA and SIMPLE materials. Relevant interactions are neutron scattering with the target nuclei and also (n,p) and (n,α) reactions in ^{35}Cl. Neutron energy thresholds on the order of 10–100 keV apply to neutron scattering; neutrons having energies as low as a few meV also induce events due to the high LET products of the above ^{35}Cl reactions.

The superheated droplet detectors (SDDs) used in SIMPLE are operated at 505 m depth (1500 mwe) in the 60 m^3 GESA facility of Laboratoire Souterrain à Bas Bruit. The reduction of environmental radon and the current α discrimination capability [2] yield neutrons as the main background source in SIMPLE measurements. The expected number of events induced by dark matter per kg of target mass per day (evt/kgd), are sufficiently low ($\ll$1 evt/kgd) that background subtraction is often required to assess the significance of a direct search measurement.

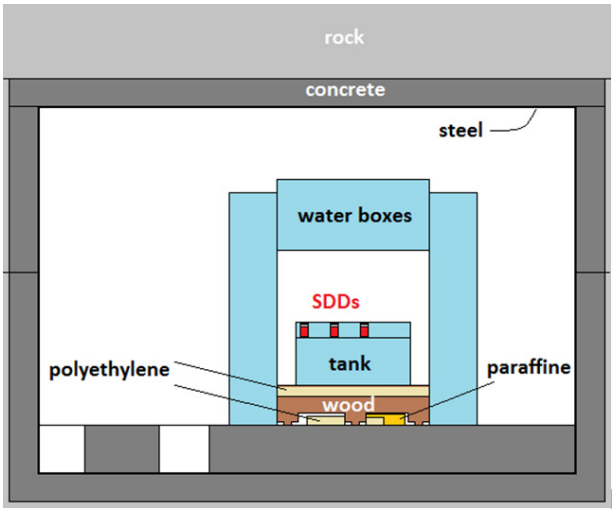

Figure 1. Geometry of the MCNP model.

The experimental characterization of such reduced neutron fields is extremely difficult (electronic noise, dose during transport, reduced efficiency, etc.). General-purpose radiation transport simulation codes based on Monte Carlo techniques are often applied to model the experiment site and the detector response [3]. Whereas neutron interactions are well-described within the code, the accuracy of the final result reflects the quality of geometry, material and neutron emitter descriptions.

The application of the MCNP code [4] to the evaluation of the initial SIMPLE set-up (Phase I) evidenced the need for a background level reduction. The neutron shield configuration used in Stage 1 of Phase II (2009–2010) [2] was improved with 10–20 cm of additional polyethylene and 10 cm of wood/paraffin, based on MCNP simulations and the material data available at the time [5]. In this work, the simulations of Stage 2 (2010–2011) [1] are supported by a set of additional radioassays and material analysis specifically performed towards the accuracy enhancement of SIMPLE Phase II background estimates.

2. MCNP model

2.1 Geometry

Figure 1 shows the MCNP model of Stage 2. Floor plan dimensions are $(400 \times 564)\,\mathrm{cm}^2$. The ceiling has a semi-cylindrical shape, the room height varying between 212–305 cm. The surrounding rock is calcite. Room walls, ceiling and floor consist of concrete, with a wall thickness between 30–100 cm, internally sheathed by a 1 cm thickness of iron forming a Faraday cage.

Each SDD consists of a 900 ml gel matrix with 12–20 g freon suspension, contained in a square glass (borosilicate Schott) of 12 cm height. Fifteen SDDs are installed in a water bath inside a $(95 \times 120 \times 65)\,\mathrm{cm}^3$ tank. The tank sits on a wooden support structure 20 cm thick. In the original, non-shielded configuration, the detectors were positioned directly over the tank floor. In Stage 1, the shielding consisted of 50 cm water in the tank, and a "castle" of 20 liter water boxes $(22 \times 25 \times 38)\,\mathrm{cm}^3$ installed around and above the tank to produce a water thickness of 50–75 cm. In addition, the detectors were raised 50 cm above the tank floor. Some water boxes were slightly deformed due to weight loading, leading to gaps in the lateral shield. In Stage 2, further attenuation of neutrons from the concrete floor

Table 1. Material data.

Material	Density ($g\ cm^{-3}$)	Composition (wgt. %)	^{238}U ($Bq\ kg^{-1}$)	^{232}Th ($Bq\ kg^{-1}$)
Rock	2,61	$CaCO_3$ (99,7%)	5,0	0,16
Concrete	2,39	$CaCO_3$ (55,4%) SiO_2 (37,2%) Al_2O_3 (3,6%) Fe_2O_3 (1,4%	10,5 10,5	7,7 7,7
Wood	0,51	H (5,8%) C (47,6) O (46,0)	0.11	3×10^{-3}
Glass	2,23	SiO_2 (81,8%) B_2O_3 (12,4%) Na_2O (2,0%) K_2O (1,5%) Al_2O_3 (2,3%)	2,74	1,27
Steel	7,874 (assumed)	Fe (assumed)	36×10^{-3}	13×10^{-3}
Water	1 (assumed)	H_2O (assumed)	32×10^{-3}	5×10^{-5}
Paraffine	0,82	$C_{25}H_{52}$ (assumed)	<0,25	<0,41

was achieved with 10–12 cm paraffin and polyethylene blocks under the tank. Water boxes were rearranged in order to eliminate the vertical gaps across the shield.

2.2 Materials

2.2.1 Composition

Chemical analyses yielded the composition of rock and concrete. Ion beam techniques were used to quantify hydrogen in the wood and boron in the glass (elastic recoil detection, and nuclear reaction analysis + elastic backscattering, respectively). Standard compositions were used for the remaining materials. The densities of most materials were measured. The results for selected materials are presented in Table 1, where composition is reported for minerals or elements with a weight fraction larger than 1%.

2.2.2 Radioassays

U and Th in the rock, concrete, steel and gel were quantified by low-background γ-spectroscopy, in which decay-related gamma-emitting isotopes are measured. Water and wood were analyzed via α-spectroscopy, allowing the direct measurement of various U and Th isotopes. For glass, polyethylene and paraffin, comparative neutron activation analysis (NAA) was employed. The results are included in Table 1.

In the cases of steel, water and wood there is a clear absence of equilibrium in the natural decay chains of ^{238}U and ^{232}Th, induced by the steel smelting and by the reduced solubility of Th in water. The analysis of the results for steel, based on the available information, is not trivial and required some approximation to set the ^{238}U and ^{232}Th levels used in the simulations. For wood and water, secular equilibrium was assumed considering the measured ^{238}U and ^{232}Th activities. The NAA results also assume secular equilibrium conditions, similarly occurring in the reference material used in the comparative method.

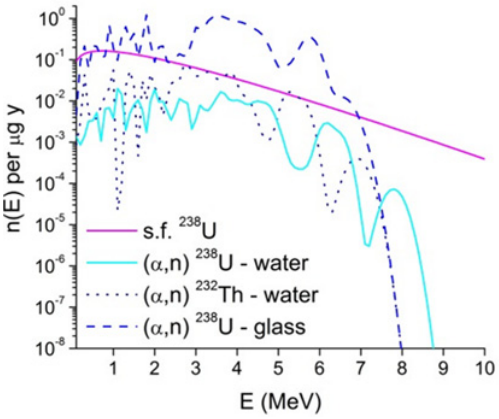

Figure 2. Neutron source spectra.

2.2.3 Neutron source

The Watt-Cranberg expression was used to describe the energy distribution of spontaneous fission (s.f.) neutrons. The Watt fission parameters, spontaneous fission probabilities and neutron multiplicity are obtained from a recent compilation [6].

Spectra and yields of (α,n) neutrons originating from each material were obtained from tabled data [7] assuming secular equilibrium within the decay series. Figure 2 illustrates the strong variation of the yield and energy distribution of s.f. and (α,n) neutrons with the material composition.

2.3 Event rate calculation

The recoil energy threshold for producing an event is 8 keV, setting conditions on the energy of neutrons (E) capable of inducing an event: $E > 401$ keV for scattering in C; $E > 75$ keV for scattering in Cl; $E > 43$ keV for scattering in F; no conditions for (n,p) and (n, α) in ^{35}Cl.

The general equation describing the reaction rate (R) for each relevant reaction is

$$R = N \int_{\mathrm{E}} [\sigma(\mathrm{E})\phi(\mathrm{E})\varepsilon_i(\mathrm{E})]\mathrm{dE} \tag{1}$$

where N is the number of target atoms per unit mass, ϕ is the neutron fluence rate in the gel volume and σ and ε the reaction cross section and detection efficiency. Neutron spectra in each SDD were calculated using the F4 tally (track length estimator) of MCNP to determine the average neutron fluence rate in the gel volume. The output is given as a histogram in a user-defined energy structure (3 bins per decade). In this case, Eq. (1) is replaced by a sum over the energy bins

$$R = N\Sigma_{\mathrm{i}}(\sigma_{\mathrm{i}}\phi_{\mathrm{i}}\varepsilon_{\mathrm{i}}) \tag{2}$$

where ϕ_{i} is the group neutron fluence rate, and σ_{i} and ε_{i} are the average reaction cross section and detection efficiency for the i-th energy bin of the simulations output, respectively. The average cross section and efficiency, which establish the equivalence between the integral and the sum, were determined after pointwise data condensation using the FLXPRO program [8]. The reaction cross sections were obtained from the ENDF/B-VII.1 library [9]. The efficiency curve for scattering reactions was obtained from [2], while for the (n,p) reaction a step function was used. It has been assumed that in each neutron interaction the maximum energy transfer from the neutron to the recoiling atom or to the reaction product will take place.

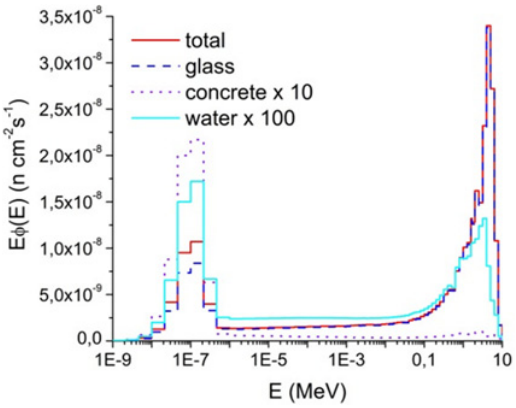

Figure 3. Calculated neutron spectra.

Table 2. Calculated event rates in evt/kgd.

Material	Phase I (non-shielded)	Phase II Stage 1	Phase II Stage 2
Concrete	5,18	w/o gaps: $9,41 \times 10^{-3}$ through gaps: 0,645	$2,89 \times 10^{-3}$
Steel	$2,22 \times 10^{-3}$	∼0	∼0
Gel	$5,42 \times 10^{-4}$	$5,38 \times 10^{-4}$	$5,38 \times 10^{-4}$
Glass	0,333	0,327	0,328
Water	$1,52 \times 10^{-3}$	$2,54 \times 10^{-3}$	$2,53 \times 10^{-3}$
Wood	$3,50 \times 10^{-3}$	$2,17 \times 10^{-5}$	$6,68 \times 10^{-6}$
Polyethylene+Paraffine	0	0	$8,44 \times 10^{-5}$
Total	5,5	0,98	0,33
Measured	–	0,74	0,15

3. Results

3.1 Neutron spectra

Figure 3 shows the calculated neutron spectrum (average over 15 SDDs) for Stage 2. It consists of a fast (1–10 MeV) spectrum significantly degraded as neutrons scatter on their way to the tallying volume and finally reach thermal equilibrium with the surrounding atoms, originating the Gaussian distribution at low energies (<1 eV). In this regard, the neutron spectrum is essentially similar to that present in a moderated nuclear fission reactor.

3.2 Event rates

The contribution of various materials to the overall event rate in the various configurations of SIMPLE is shown in Table 2. In Stage 1, the gaps (1 cm thickness) in the water shield were considered. The statistical uncertainty in each result is smaller than 3%.

The results show that a significant decrease of the neutron background originating from concrete has been accomplished through the implementation of the water shield and latter improvements, namely the elimination of shield gaps. This reduction was largely compensated by small increases in the event rate induced by the shielding itself.

In the final configuration, the borosilicate glass employed in the gel-containing flasks is responsible for ∼98% of the neutron-induced signal. This effect is caused by the significant ^{238}U and ^{232}Th contamination of glasses which, combined with the particularly high boron content of the borosilicate

glass produces an important yield of (α,n) neutrons. The glass-induced event rate has the following contributions: 12% from s.f.; 64% from (α,n) due to ^{238}U; 24% from (α,n) due to ^{232}U. In terms of inducing reactions from neutrons produced in glass, 70% of the event rate is caused by neutron scattering with F atoms in the freon. The remaining contributions are due to scattering with C (18%) and Cl (12%), while transmutation reactions produce <1%.

4. Conclusions

Through the implementation of a water-based neutron shielding, the event rate induced by the extrinsic neutron background has been reduced by 3 orders of magnitude relatively to the initial, non-shielded configuration of SIMPLE. The neutron-induced background signal in the latest configuration is 0,33 evts/kgd. The signal originates essentially in the detector container, and can be further reduced using low-activity glasses. The remaining option left at GESA is an increased water shield that decreases the concrete contribution. This effort is however justified only in the case that higher radiopurity water is used. From a comparison with measurements, it is concluded that no dark matter was observed in Phase II of SIMPLE.

We thank Dr. Christophe Emblanch (University of Avignon) for the chemical analysis of the site concrete and rock. Dr. Pia Loaiza is acknowledged for the radio-assays of concrete and steel. This work is partly funded by the Nuclear Physics Centre of the University of Lisbon, and by grants PTDC/FIS/115733/2009 and PTDC/FIS/121130/2010 of the Portuguese Foundation for Science and Technology.

References

[1] M. Felizardo et al., Phys. Rev. Lett. **108**, 201302 (2012).
[2] M. Felizardo et al., Phys. Rev. Lett. **105**, 211301 (2010).
[3] V.A. Kudryatsev et al., Eur. Phys. J. A **36**, 171 (2008).
[4] X5 Team, Los Alamos Ntl. Lab., LA-UR-03-1987 (2003).
[5] A.C. Fernandes et al., Nucl. Instr. Meth. A **623**, 960 (2010).
[6] E.F. Shores, Nucl. Instr. Meth. B **179**, 78 (2001).
[7] D.M. Mei et al., Nucl. Instr. Meth. A **606**, 651 (2009).
[8] F.W. Stallmann, Oak Ridge Ntl. Lab., ORNL/TM-9933 (1985).
[9] M.B. Chadwick et al., Nucl. Data Sheets **107** 2931 (2006).